Registration efficiency of neutron detectors of different geometry

Pletnikov E.[1,2], Yanke V.[3]

[1]*Moscow Aviation Institute (State University of Aerospace Technologies), Moscow, Russia; pev36@mail.ru,*

[2]*Institute for Nuclear Research of the Russian Academy of Sciences, Troitsk, Russia,*

[3]*Institute of Terrestrial Magnetism, Ionosphere and Radio Wave Propagation RAS (IZMIRAN), Moscow, Russia, yanke@izmiran.ru*

Abstract

A mathematical simulation of the neutron detectors response to neutron (and other secondary cosmic ray particles) flux incident on the detector has been done. Registration efficiencies of the neutron detectors of different geometries throughout the energy range of secondary neutrons has been found out.

Introduction

In spite of several decades history the neutron monitors connected in the World network are an excellent device for measuring of cosmic particles with energies > 400 MeV nowadays. The energy range of the neutron monitors are good addition and continuation of the upper boundary of energies measuring by the cosmic ray detectors. Due to high statistical accuracy the neutron monitors are capable to measure even weak anisotropy and other characteristics relating to solar and galactic cosmic rays. The estimation of cosmic ray flux variations beyond the magnetosphere according to the data from ground-level count rate measurements $N(R_c,h,t)$ can be done on the base of the famous formula

$$N(R_c,h,t) = \int_{R_c}^{\infty} \sum_{i=p,\alpha,Z} S_i(R,h)\cdot J_i(R,t)dR \,. \qquad (1)$$

Here $J_i(R,t)$ is a differential rigidity spectrum of the *i*-type particles of the primary cosmic rays, $S_i(R,h)$ is a yield function of a neutron monitor at the point with geomagnetic cutoff rigidity R_c at a depth of h in the atmosphere. The yield function of a neutron monitor is determined both by particle flux density incident on the monitor and by an efficiency of the flux registration by the detector. So the yield function can be written as

$$S_i(R,h) = S_{NM} \sum_{j=n,p,\pm\pi,\pm\mu} \cdots \iint \varepsilon_j(E,\Omega)\cdot m_{ij}(R,h,E,\Omega)dEd\Omega \,, \qquad (2)$$

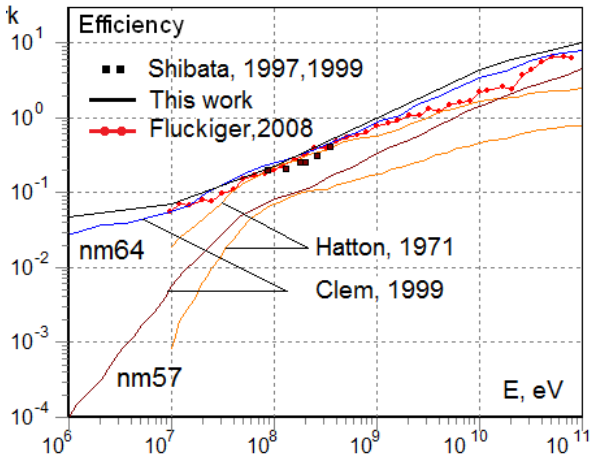

Fig. 1. Efficiency of the neutron supermonitor 6nm64 and 12nm57.

Here S_{NM} is neutron monitor area, $\varepsilon_j(E,\Omega)$ is registration efficiency of E energy particles incident on the neutron monitor on the angle θ to the vertical and azimuth angle φ. The function $m_{ij}(R,h,E,\Omega)$ is so-called integral generation multiplicity that is a number of *j*-type particles at the observation level h (or differential secondary particle flux density). These particles were generated due to nuclear cascade development in the atmosphere from the primary *i*-type particle with the rigidity R incident on the atmosphere boundary on the θ angle. From (2) it is clear how important to know a registration efficiency trend details. If to define a detector efficiency as a possibility of registration of different energies and types particles incident on the detector then the neutron detector efficiency is depend heavily on the incident particles energy. Energy characteristics of a neutron monitor are much differ from the characteristics of other detectors, for example a muon telescope efficiency is close to "one" and isn't virtually depend on incident particles.

The goals of this work are simulation of neutron detectors response to neutrons and other particles of different energies passing through device aperture and efficiencies calculation of neutron detectors of different geometries.

1 The calculation method

For determination of the efficiencies of neutron different geometries detectors the steady-state simulation of the cascades activated by the flux of incident secondary particles in the energy range from slow neutrons up to particles of 100 CeV has been carried out.

The calculations have been carried out on the base of the FLUKA 2008.3c.0 (32x) software package [1]. For this purpose the software package involving the mathematical model of neutron detectors and processes in the proportional counters has been created. Another detectors of the neutron component sensitive to incident particle flux in different energy ranges have been under consideration along with the standard neutron monitors 6nm64 [2].

The parallel monoenergetic particle flux incident on the neutron detector on various angles was under consideration. The flux cross-section was chosen of 5x5 m^2 and it was a compromise decision as from one hand environmental matter transforming the incident particle flux should be allowed for. From other hand an overincrease of the flux cross-section enhances the calculation time of each event proportionally. So the optimal cross-section is 4 times more then the monitor area. The incident particle energies were varied relating to their spectrum. The neutron source is on 30 sm height over the detector and the detector is on 1 m height from the surface. The number of events concerned is 10^5. For all the detectors the environmental and underlying surface effects were studying. The further cases of the underlying surface were allowed for: soil, water (in Antarctica, for example) and a case when soil is in the distance of several neutron paths in the air.

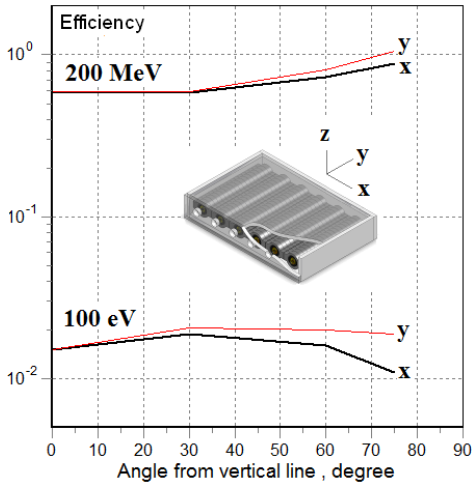

Fig. 2. The angular dependence of front (**y**) and lateral (**x**) neutron fall.

The out-put parameters of the software package are *an average energy release in the counter in a gas mass unit (dose)*. Let's identify an average ($N_0=10^5$ events) energy release in the counter in a gas mass unit as E_n (MeV/g). Allowing for that in each act of a slow neutron capture by the ^{10}B nucleus the energy of $\overline{Q}$ =2.33 MeV is released, then for a number of particles registered by the neutron monitor consisting of 6 counters it may be written as $N_{counts} = 6mE_nN_0/\overline{Q}$, where m – gas mass in one counter. In the problem $N_0=10^5$ a number of particles falls uniformly on the area S and for a number of particles incident on the neutron monitor counters it may be written as $N = \frac{N_0 \cdot S_{NM}}{S}$ allowing for that the neutron monitor area is S_{NM}. Then the detector efficiency is defined as $\varepsilon = \frac{N_{counts}}{N} = \frac{6mE_n}{\overline{Q}} \cdot \frac{S}{S_{NM}}$. Sometimes the effective detector area defining as $S_{NMeff} = S_{NM}\varepsilon$ is made use of .

2 The standard neutron monitor efficiency

The standard 6nm64 neutron monitor efficiencies obtained in the wide range of energies up to 100 GeV are in Fig. 2. In the same range of energies the 6nm64 neutron monitor efficiencies were calculated only in the former work [3] on the base of FLUKA package. The efficiency comparison shows (Fig. 1) that our results are just over the results of the work [3] and a distinction is increasing with energy decrease of incident particles. Maybe it is related to the later FLUKA package application in this work where neutron moderating processes are allowed for more correctly. A good agreement of efficiencies resulted with other calculating and experimental efficiencies of the detectors with counting rate determining just by the same energy range (Fig. 3-6) may be some evidence.

In the energy range higher then the cut off energy (> 10 MeV) by the reflector due to neutron albedo there are several calculating and experimental works on the determining of the neutron monitor efficiency. In Fig. 1 there are results of the primary Hatton work [4] and results of one of the latest Fluckiger works [5] obtained by Geant4 modeling. It is seen the scatter is wide enough. In Fig. 1 there is the only experimental result of the Shibata's work [6] obtained due to raying of the 1nm64 neutron monitor by the neutron flux of energies from 100 up to 400 MeV on the accelerator. In this energy range the agreement of calculating and experimental data is a lot better.

In Fig. 2 the angular dependence for front and lateral neutron fall is shown. Expectedly due to a strong neutrons diffusion within the neutron monitor volume the efficiency angular dependence is very weak in all cases and it makes possible to restrict oneself by the effective value of the efficiency.

3 The efficiencies of slow, epithermal and fast neutrons detector

For some scientific and applied problems the neutron monitors without lead multiplicator are used (Fig. 3-6). Such detectors' configuration aren't standardized. For example, at the South Pole station and at Sanae the lead-free neutron monitors are made use of. For example, at Sanae station [7] the 4nm64D monitor made of boric counters is running and the detector configuration is near to the standard nm64 neutron monitor configuration consisting of 4 counters. For monitoring of the moisture deposit the lead-free neutron monitors with small area made of 65NH45 helium counters (Ø25Х 450мм) surrounded only by polyethylene moderating medium are used [8]. Some researches of geophysical effects (seismic, thunderstorm) are based on the slow neutron detectors [9-11] of different configurations. But every detector consists of a counters set, moderator and reflector differing only by sizes.

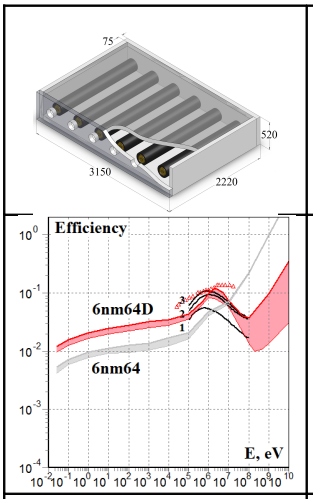

Fig. 3. Lead-free neutron supermonitor with the reflector 6nm64D: configuration and efficiency.

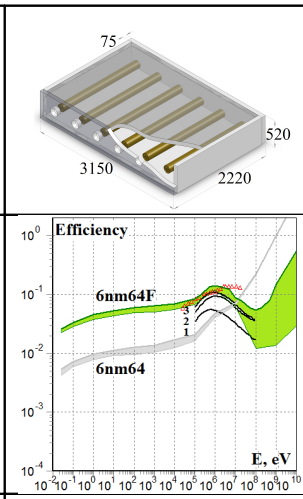

Fig. 4. Lead-free neutron supermonitor with the reflector 6nm64F: configuration and efficiency.

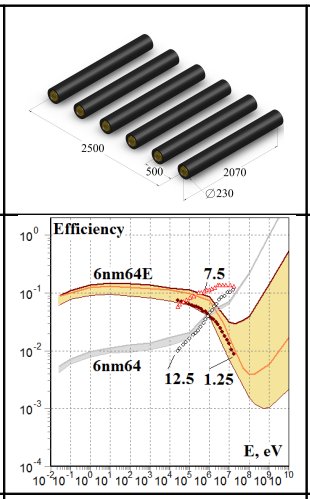

Fig. 5. Neutron supermonitor without the reflector 6nm64E: configuration and efficiency.

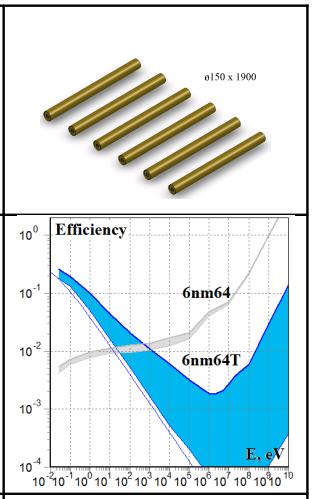

Fig. 6. Slow neutron detector 6nm64T from 6 boric counters CHM-15: configuration and efficiency.

In selecting the neutron monitor geometry without a breeder we issued from the standard neutron monitor geometry as just the same detectors are made use of in IZMIRAN. In lead absence (Fig. 3) or by exclusion of the tube-moderator surrounding the counter (Fig. 4) we get detectors with characteristics differing insignificantly. Such detectors are the most sensitive to fast neutrons. If detector consists only of the counters surrounding by a tube-moderator we get lead-free neutron monitor (Fig. 5) but with considerably different characteristics. Such detector is very sensitive to epithermal neutrons. If the counters are only used we come to the slow neutron detector (Fig. 6). It is clear another size detectors (the reflector and moderator thickness first of all) can be of some other features but the differences are not principle and this requires new calculations in the every case.

In Fig 3-6 there is a dependence of the efficiency from the incident neutron energy for lead-free detectors of 4 types. In each case the dedicated area is bounded by two curves. The upper curve is for over-ground detector, the lower curve is for far-from-soil detector. From the crosshatched region it is seen that in a case of the standard 6nm64 neutron monitor surrounding mass effects as a minimum, and in other cases it effects appreciably especially for reflector-free detector. There is also efficiency for the 6nm64E detector for its being on the ice, for example in Antarctica. At the high energies and far from soil the efficiency is increasing again after the minimum due to a cascade development in the air. The calculations provide support for this when the air density is three times less.

Let's compare with other results. In [12] the efficiency of the detector consisting of 1-3 rows of CHM15 counters on 6 counters in a row was calculated. The group of counters is surrounded by the common reflector with wall thickness of 70 mm. Such configuration is closed mostly to the 6nm64D or 6nm64F detectors. In Fig. 3 and 4 there is a comparison of efficiencies calculated and obtained in [12] for the cases of 1, 2 or 3 layers of

counters (numbers of curves). The agreement is good both by the absolute value and for the position of efficiency maximum.

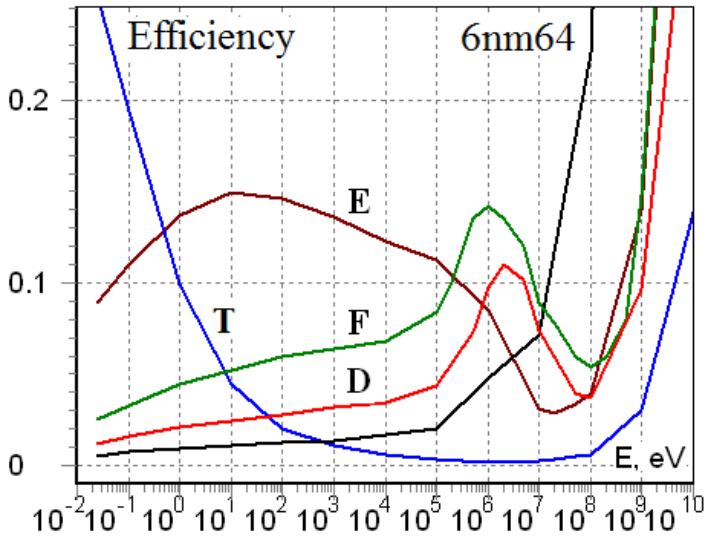

Fig. 7. Comparison of the neutron detectors efficiencies.

In [13] the efficiency of the detector consisting of a single neutron counter NW G-15-34A and a paraffin moderator surrounding it was calculated. Three moderator thicknesses 1.25, 7.5 and 12.5 cm were under consideration. The result is in Fig. 5. The detector with paraffin moderator thickness of 12.5 sm is the nearest to the 6nm64E detector with moderator thickness of 2.4 cm. Some ambiguity in absolute values of the efficiency appears due to different geometric sizes of the usable boric counters NW G-15-34A and CHM15. But the efficiency trend in the range of 0.1-10 MeV (1.25 curve) is in good agreement with our results. Besides the curve 7.5 in the same energy range agrees in amplitude satisfactorily with the detectors efficiencies trend in Fig. 3 and 4 (triangles curve).

In Fig. 6 there is the efficiency of 6nm64T detector consisting of 6 single counters dispersed. For the comparison there is a single counter efficiency calculated on the assumption that the effective cut-off dependence from the neutron energy for the boric counters is $\sigma = 738E^{-1/2}$ barn (the curve lower the dedicated area). The mismatch of this curve with the lower one is related to some air effect round the detector.

		D	F	E	T
<ε>, %	Not Ground	5.0	7.3	4.3	0.4
	Ground	6.7	10.3	9.1	1.3
<E>, MeV	Not Ground	11.4	7.7	1.2	1.1
	Ground	63	62	67	81

Table 1. Average efficiency and average energy for the neutron detectors of different types.

Efficiencies comparison of all the neutron detectors concerned above for the case of detector with soil underlayer is in Fig. 7. The energy range of various detectors (of slow (T), epithermal (E) and fast (F) neutrons) is seen well. A particle contribution to the counting rate over several decades of MeV for all the detectors is related to the environment influence. And as it is seen in Fig. 7 it may be essential. Integral detector efficiency is determined as $\langle \varepsilon \rangle = \int_{E_0}^{\infty} \varepsilon(E) D(E) dE \Big/ \int_{E_0}^{\infty} D(E) dE$ where $D(E)$ is a spectrum of neutrons incident on the monitor. Average efficiencies and average energies of registering particles for various neutron detectors are in the Table 1.

Conclusions

In the wide range of energies from slow neutrons up to fast ones the efficiencies for neutron detectors of different configurations were calculated. There is a good agreement of our results with the available experimental and calculating data of other authors both by the absolute value and for the efficiencies and energy.

A particle contribution to the counting rate over several decades of MeV for all the lead-free detectors is related to the environment influence and can exceed the main flux contribution.

Acknowledgements

This work is partly supported by Program No 6 BR of the Presidium RAS “Neutrino Physics and Astrophysics” .

Literature

[1] *Ferrari A., P.R. Sala, A. Fasso, J. Ranft.* FLUKA: a multi-particle transport code.// CERN 2005-10. 2005. INFN/TC_05/11, SLAC-R-773, (Fluka-2006) REALEASE-NOTES.fluka2008.3c,. FRLUKA http://www.fluka.org/, the official site, 2008.

[2]. *Hatton C.J. and Carmichael H.* Experimental investigation of the nm-64 Newtron Monitor. //Can. J. of Phys., v. **42**, 2443-2472, 1964.

[3] *Clem J. M.* Atmospheric Yield Functions and the Response to Secondary Particles of Neutron Monitors.// Proc. 26th ICRC, Salt Lake City, Vol. 7, p. 317, 1999; *Clem J. M., L. I. Dorman.* Neutron Monitor Response Functions. // Space Science Reviews 93, 335–359, 2000.

[4] *Hatton C. J.* The Neutron Monitor. // American Elsevier Publishing Company. New York. 1971.

[5] *Fluckiger E.O., M.R. Moser, B. Pirard, R. Butikofer, L. Desorgher*. A parameterized neutron monitor yield function for space weather applications. // Proceedings of the 30th ICRC. Mexico. Vol. 1. p. 289–292. 2008.

[6] *Shibata S., Y. Munakata, R. Tatsuoka Y. Muraki, Y. Matsubara, K. Masuda, T Koi, T. Sako, A. Okada, T. Murata, H. Tsuchiya, I. Imaida, T. Hoshida Y. Kato, A. Yuki, S. Ohno K. Hatanaka, T. Wakasa H. Sakai, T. Nonaka, T. Ohnishi Y. Ishida*. Calibration of Neutron Monitor using Accelerator Neutron Beam. // Proc. 26th ICRC. Salt Lake City. 7. 313. 1999; Nucl. Instrum. Methods Phys. Res. A. 463. 316. 2001.

[7] *Stoker, P.*. Primary spectral variations of cosmic rays above 1 GV, // 17th ICRC. Paris. v.3. p.193-196. 1981.

[8] *Paquet E, Laval M., Белов А.В., Ерошенко Е.А., Kartyshov V.G., Янке В.Г.*. An Application of Cosmic-Ray Neutron Measurements to the Determination of the Snow Water Equivalent. // Proc. 30th ICRC. Mexico. v.1. 761-764. 2008.

[9] *Antonova V.P.,Kryukov S., Chubenko A., Shlyugaev Yu., Schepetov A.* Influence of the surface electric field variations on the neutrons registration due to weather. // Proc. of the 31st RCRC, Moscow, 2010.

[10] *Kozlov V.I., Mulayarov V.A., Starodubtsev S.A., Toropov A.A.* Variations of the neutrons and muons produced by the cosmic rays in the atmosphere and thunder lectric fields. // Proc. of the 31st RCRC, Moscow, 2010.

[11] *Antonova V.P., Volodichev N.N., Kryukov S.V., Chubenko A.P., Schepetov A.L.* Results of the slow neutrons detecting at Tien Shan high-altitude station. // Geomagnetism and aeronomy. Vol. 49, № 6, pp. 798-804, 2009.

[12] Luzov A.A., Matyukhin Yu.G., Sdobnov V.E. Energy dependence of the neutron monitor nm64. // Col. " Research on geomagnetism and aeronomy and Solar physics", M. Nauka, Iss. 20, 356, 1971.; Pakhomov N.I., Sdobnov V.E. Calculation of the neutron supermonitor characteristics. // Col. " Research on geomagnetism and aeronomy and Solar physics", M. Nauka, Iss. 42. 185. 1977; *Sdobnov V.E.*. Spectral sensitivity of the neutron monitor without lead for different geometries of the instrument. // Proc 16th ICRC. Kyoto. v.4. 368. 1979.

[13] *Hess W.N., Patterson H.W., Wallace R.*. Cosmic ray neutron energy spectrum. // Phys. Rev. 116. 445-457. 1959.

[14] *Hughes E.B., Marsden P.L., Brook G., Meyer M.A., Wolfendale A.W.*. Neutron production by cosmic, ray protons in lead. //Proc. phys. soc. v. 83. p. 239—251. 1964.

[15] Maurchev E.A., Gvozdevsky B.B., Balabin Yu.V., Vashenyuk E.V. Modeling of the neutron monitor response function.// Proc. of the 31st RCRC, Moscow, 2010.